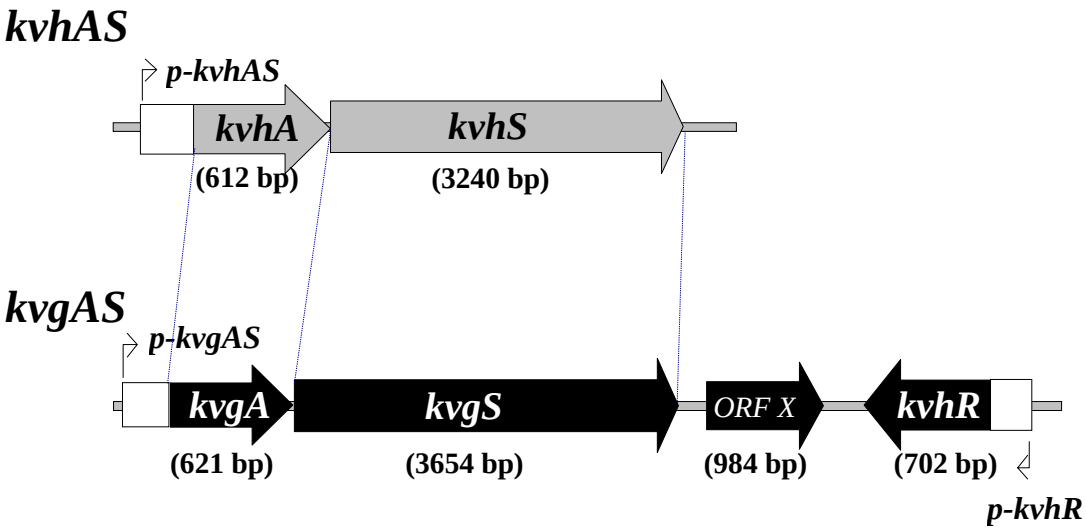

Fig. 1. Schematic diagram of the homologous two-component systems *kvhAS*, *kvgAS* and *kvhR* of *K. pneumoniae* CG43. The deduced amino acids of *kvhA* has 58.5 % and 57.0 % similarity with that of *kvgA* and *kvhR* respectively, and the deduced amino acid of *kvgA* has 55.5 % similarity with that of *kvhR*. The putative promoter regions *P-kvhAS*, *P-kvgAS* and *P-kvhR* were depicted as open boxes. The arrowheads indicate the direction of the transcripts.

A. Growth curve

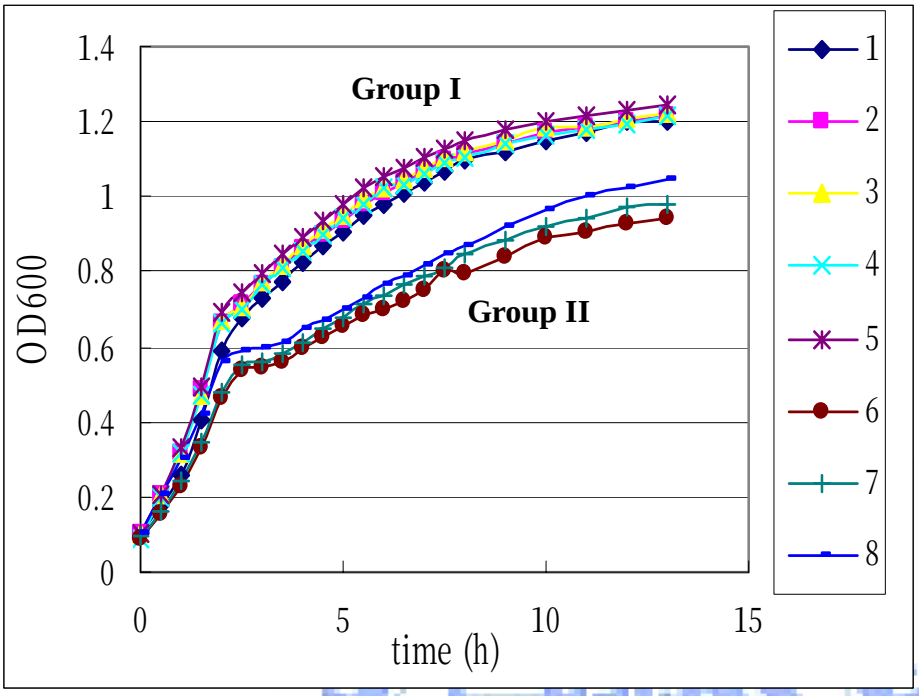

B. Sedimentation test

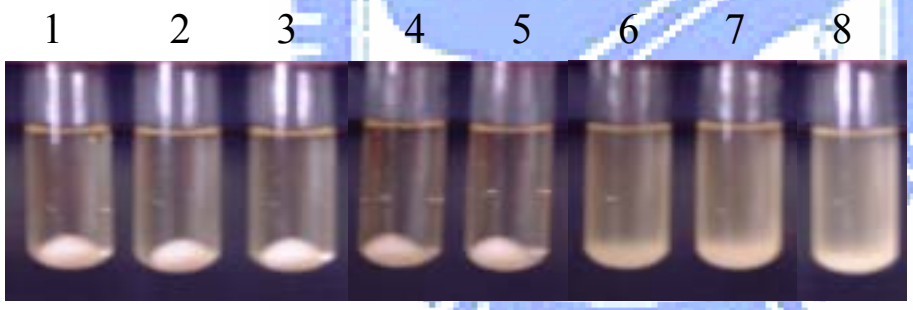

Fig. 2. The growth curve (A) and sedimentation test (B) of a series of mutants derived from LacZ16. The strains tested were cultured in LB broth at 37°C and subjected to centrifugation at 4,000 rpm (1,500 *g*) for 3 min. According to collective analysis of both assays, two groups can be identified, in which the Group I includes 1: *kvgA*$^-$, 2: *kvhR*$^-$, 3: *kvhA*$^-$*kvgA*$^-$, 4: *kvgA*$^-$*kvhR*$^-$ and 5: *kvhA*$^-$*kvgA*$^-$*kvhR*$^-$, and Group II contains 6: LacZ16, 7: *kvhA*$^-$ and 8: *kvhA*$^-$*kvhR*$^-$.

A. Growth curve

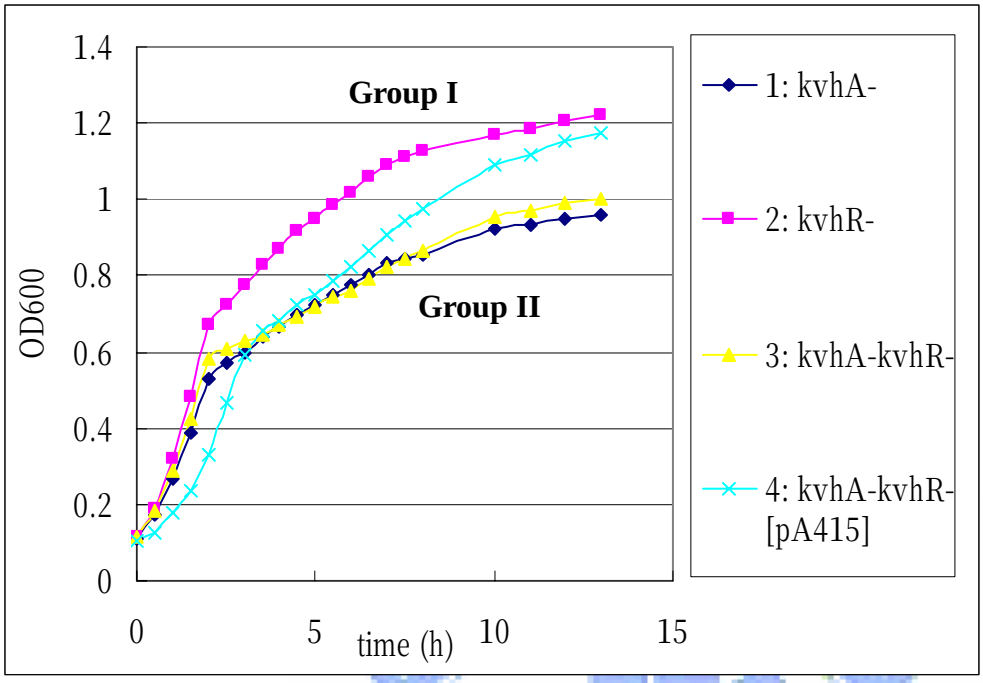

B. Sedimentation test

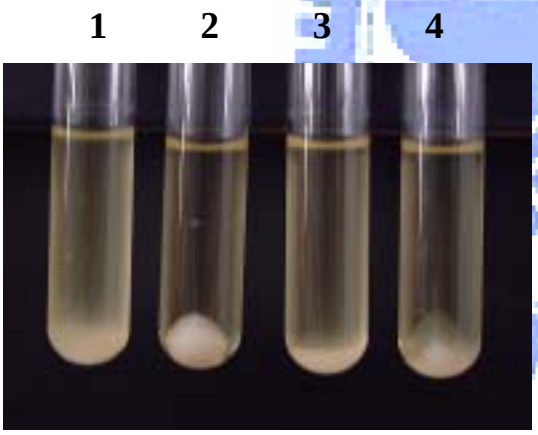

1: *kvhA*$^-$
2: *kvhR*$^-$
3: *kvhA*$^-$*kvhR*$^-$
4: *kvhA*$^-$*kvhR*$^-$[pA415]

Fig. 3. Complementation of *kvhA*$^-$*kvhR*$^-$ with a *kvhA* recovers both growth (A) and phenotype (B) to the same as that of *kvhR*$^-$. The plasmid pA415 was derived from pRK415, which contains the *kvhA* with its putative promoter region.

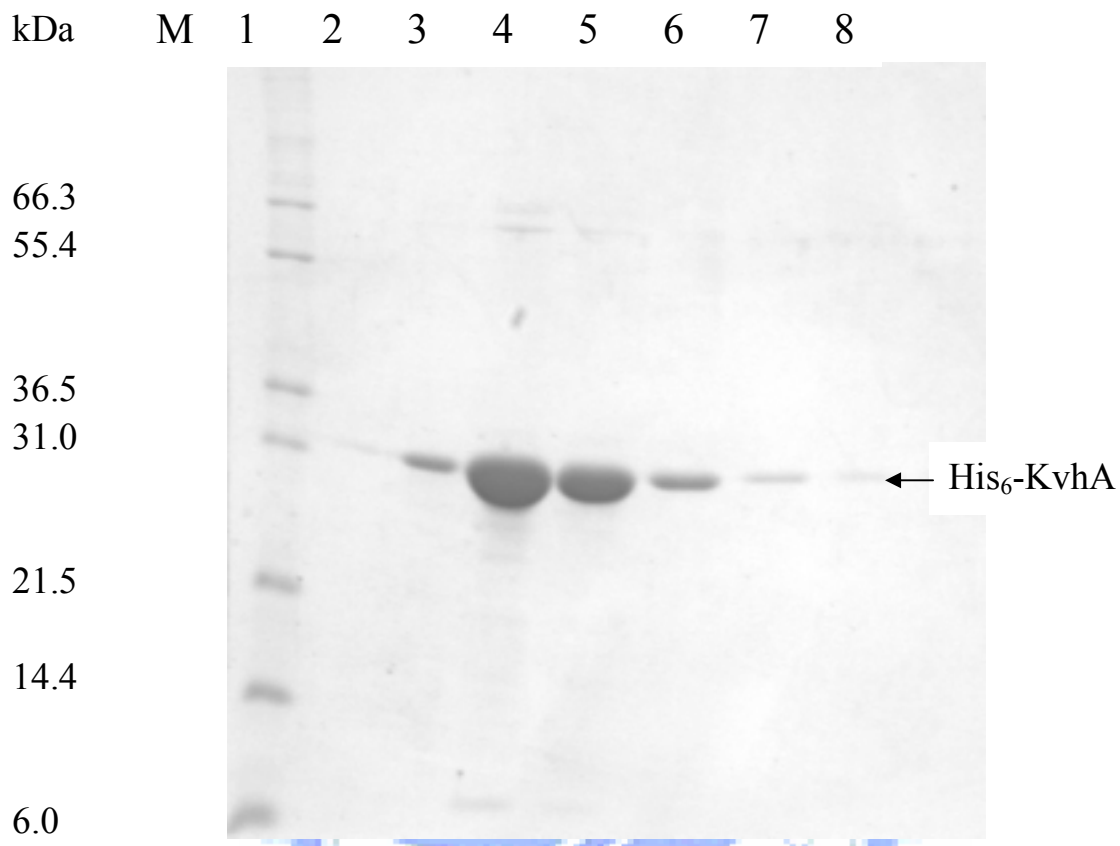

Fig. 4. Purification of the His_6-KvhA recombinant protein using His-nickel-nitrilotriacetic acid column (Ni-NTA) affinity chromatography. According to this SDS-PAGE, the His_6-KvhA, as indicated by an arrow, has a molecular weight of 28 kDa. Lane M, protein MW marker; the Lanes 1~8 are the eluted-fractions through the His-tag affinity chromatography. The arrow indicates the purified His_6-KvhA.

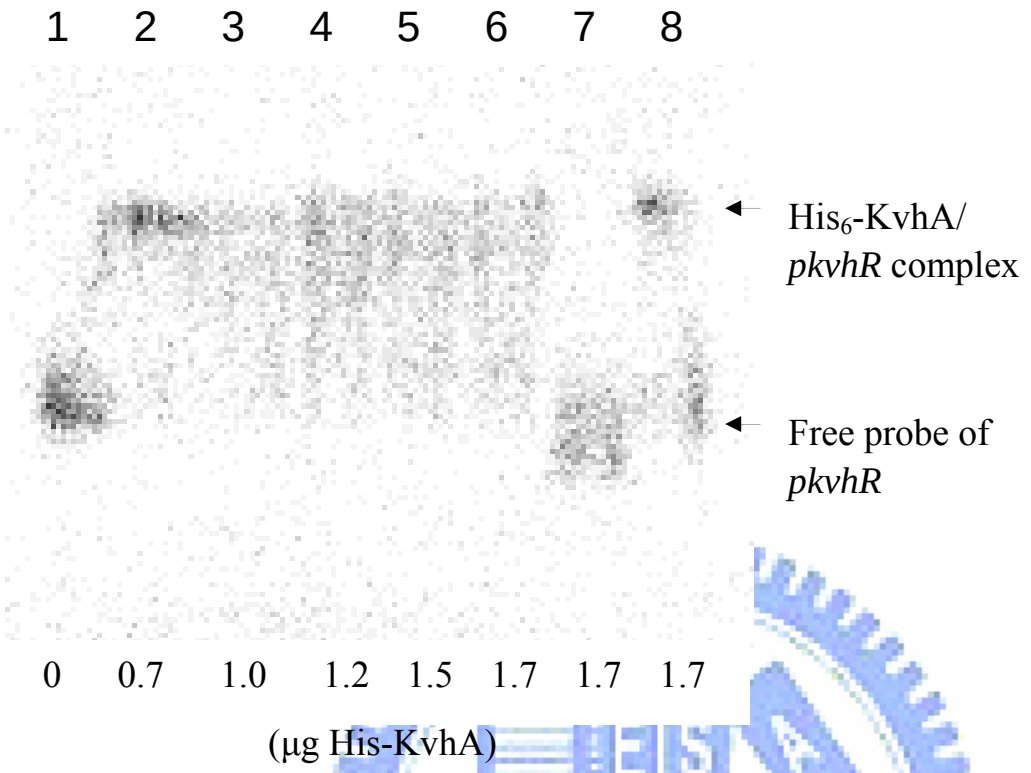

Fig. 5. The His_6-KvhA bound specifically to P_{kvhR} in electrophoretic mobility shift assay. The ^{32}P-labeled P_{kvhR} was incubated respectively with an increasing amount of His_6-KvhA as indicated. Lanes: 1, no protein added; 2, 0.7 μg of protein; 3, 1.0 μg of protein; 4, 1.2 μg of protein; 5, 1.5 μg of protein; 6 to 8, 1.7 μg of protein. Inhibition of the specific competition is shown in lane 7 by adding an excess amount of unlabeled P_{kvhR}. The specific binding was also demonstrated by adding excess amount of non-specific competitive pUC19 DNA in lane 8.

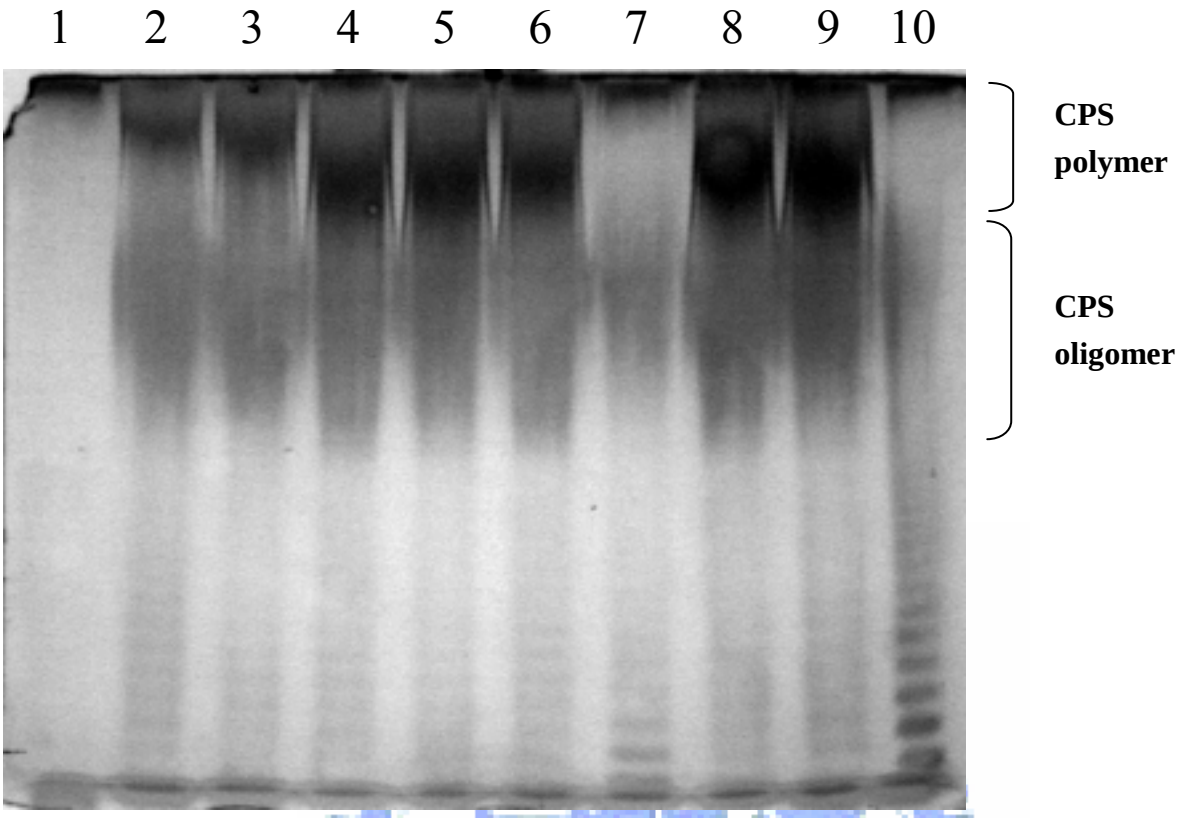

Fig. 6. CPS production patterns analyzed by Alcian Blue-silver staining after 10% (w/v) polyacrylamide gel electrophoresis. The CPS was isolated from *K. pneumoniae* strains grown overnight at 37℃ in LB and purified with hot phenol. Lanes: 1, U9451; 2, LacZ16; 3, *kvhA*$^-$; 4, *kvgA*$^-$; 5, *kvhR*$^-$; 6, *kvhA*$^-$*kvgA*$^-$; 7, *kvhA*$^-$*kvhR*$^-$; 8, *kvgA*$^-$*kvhR*$^-$; 9, *kvhA*$^-$*kvgA*$^-$*kvhR*$^-$; 10, *kvhA*$^-$*kvhR*$^-$[pA415]. The CPS polymer with high molecular weight and the smaller CPS oligomer are indicated.

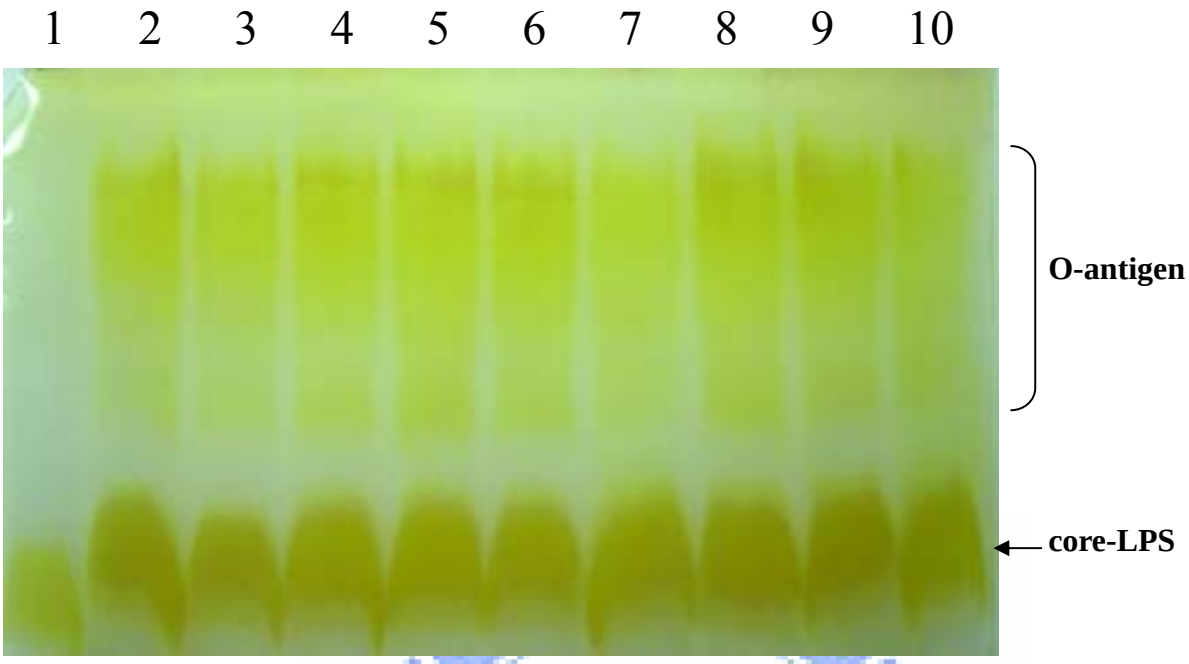

Fig. 7. Silver staining of a LPS separated by 15% (w/v) SDS-PAGE. The LPS was isolated from *K. pneumoniae* strains as same as CPS purification. Lanes: 1, U9451; 2, LacZ16; 3, *kvhA*$^-$; 4, *kvgA*$^-$; 5, *kvhR*$^-$; 6, *kvhA*$^-$*kvgA*$^-$; 7, *kvhA*$^-$*kvhR*$^-$; 8, *kvgA*$^-$*kvhR*$^-$; 9, *kvhA*$^-$*kvgA*$^-$*kvhR*$^-$; 10, *kvhA*$^-$*kvhR*$^-$[pA415]. The O-antigen was indicated by a bracket and core-LPS was indicated by an arrow.

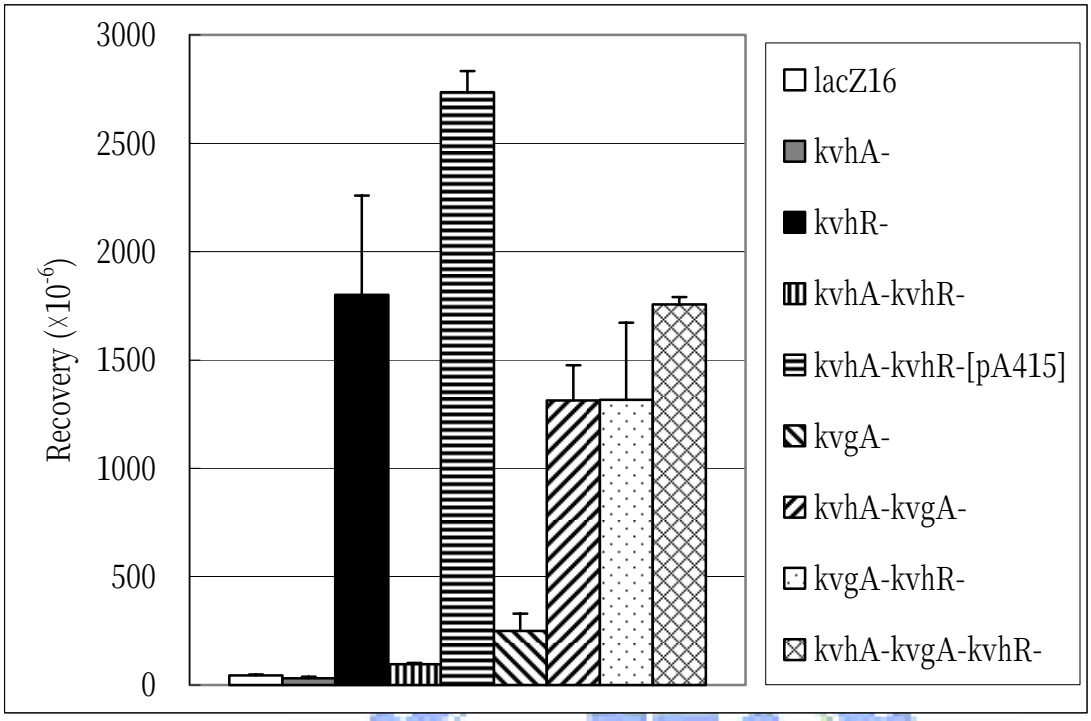

Fig. 8. Anti-phagocytosis activity of the mutants derived from *K. pneumoniae* LacZ16 using THP-1 macrophage cell line. After incubated a 30 : 1 ratio of bacteria to macrophage for 2 h, the cells were washed by PBS and treated with Gentamycin (100 μg/ml) to remove excess bacteria. The ingested bacteria were quantified by plating onto LB agars. Recoveries are shown as the ratio of ingested bacteria (CFU) / initially incubated bacteria (CFU). The mean and standard deviation were calculated from three independent experiments.

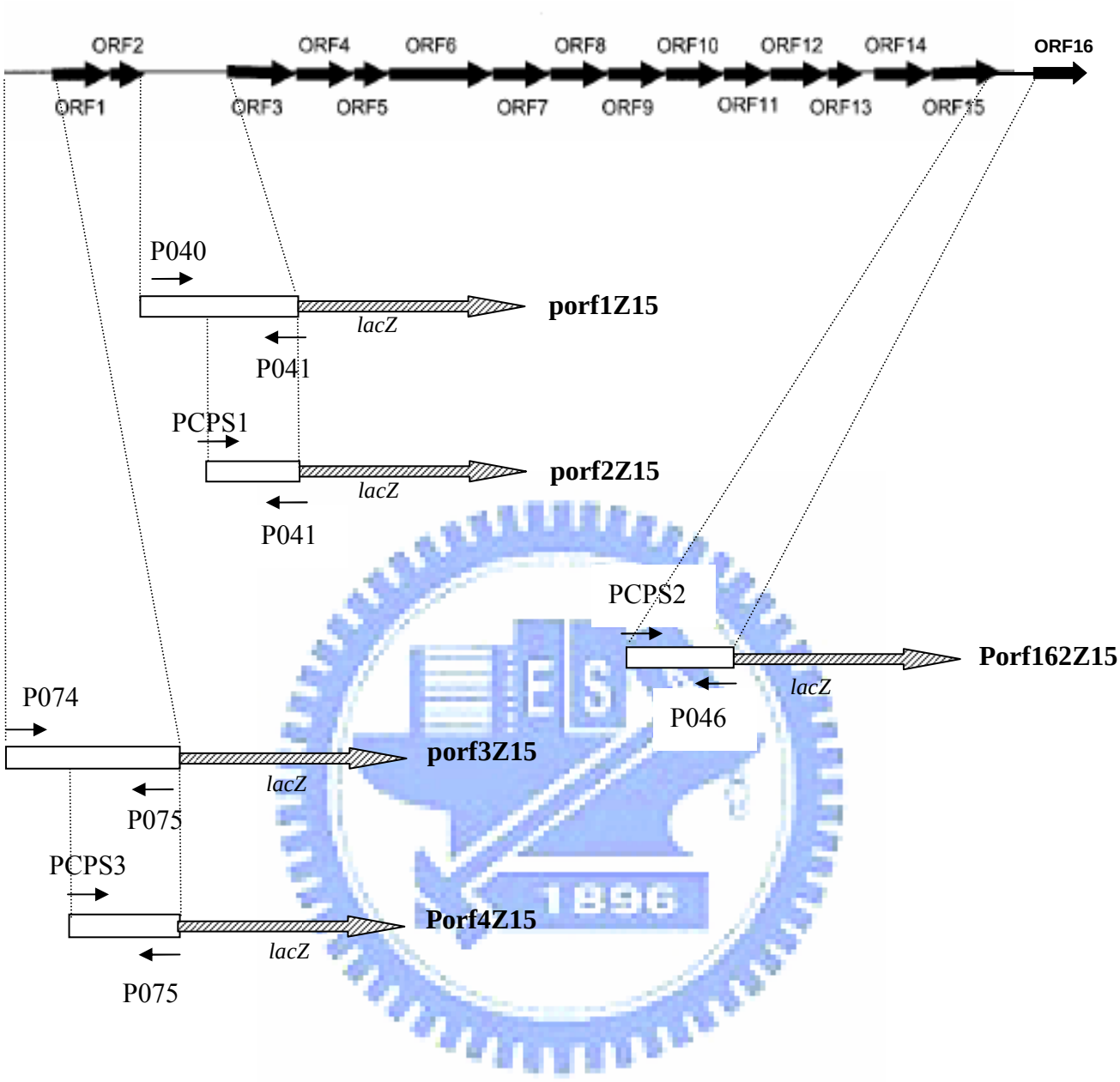

Fig. 9. The putative promoter regions of *K. pneumoniae* K2 *cps* gene cluster were cloned into placZ15 as *lacZ* transcriptional fusions. The primers used for PCR amplification and the extents of subclones used in this study are indicated. porf1Z15 and porf2Z15 ($P_{orf1\text{-}2}$*::lacZ*) comprise the regions controlling the expression of *orf1* and *orf2*, porf3Z15 and porf4Z15 ($P_{orf3\text{-}15}$*::lacZ*) carry the putative promoter regions responsible for initiating transcription of the operon containing *orf3* to *orf15*, and porf162Z15 ($P_{orf16\text{-}17}$*::lacZ*) contains the putative promoter region of *orf16* and *orf17*.

(A)

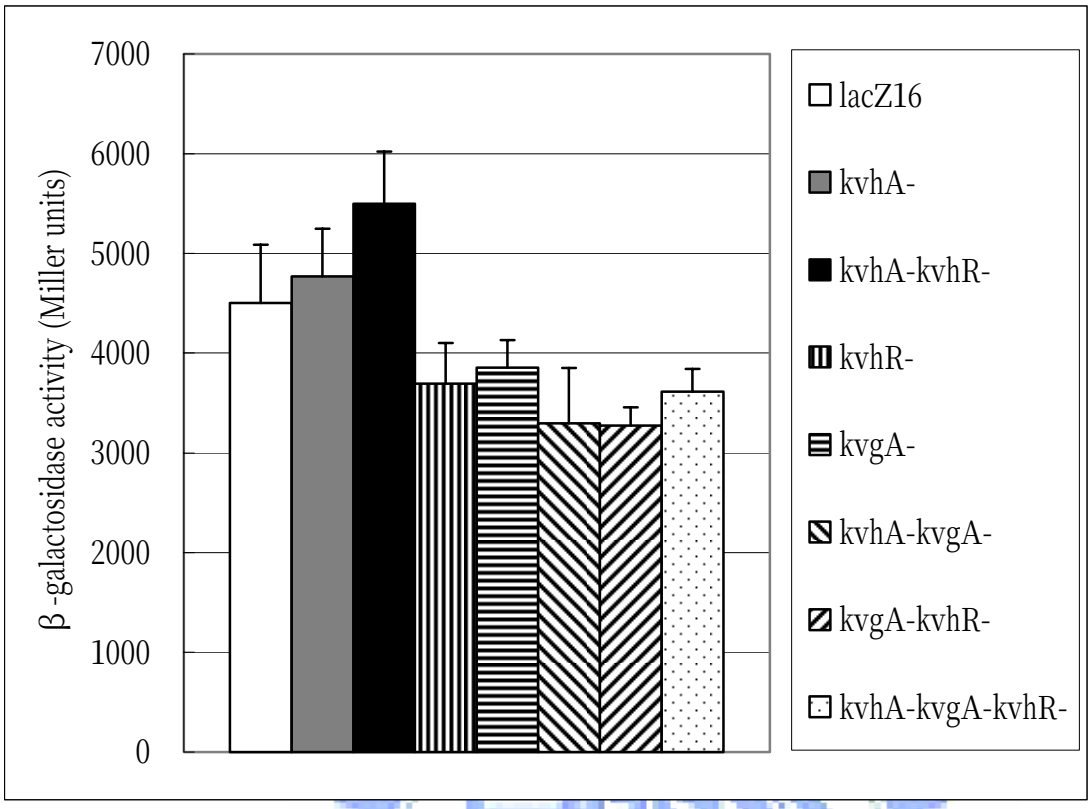
β -galactosidase activity (Miller units)
7000
6000
5000
4000
3000
2000
1000
0
lacZ16
kvhA-
kvhA-kvhR-
kvhR-
kvgA-
kvhA-kvgA-
kvgA-kvhR-
kvhA-kvgA-kvhR-

(B)

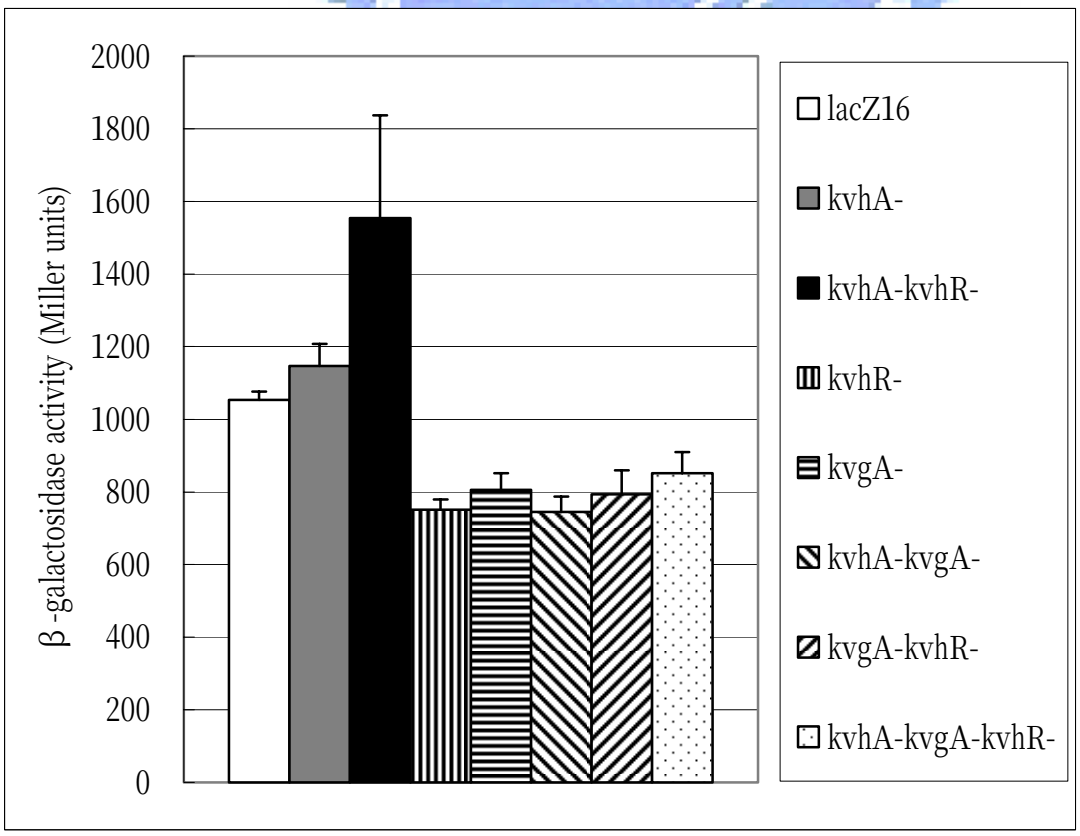
β -galactosidase activity (Miller units)
2000
1800
1600
1400
1200
1000
800
600
400
200
0
lacZ16
kvhA-
kvhA-kvhR-
kvhR-
kvgA-
kvhA-kvgA-
kvgA-kvhR-
kvhA-kvgA-kvhR-

(C)

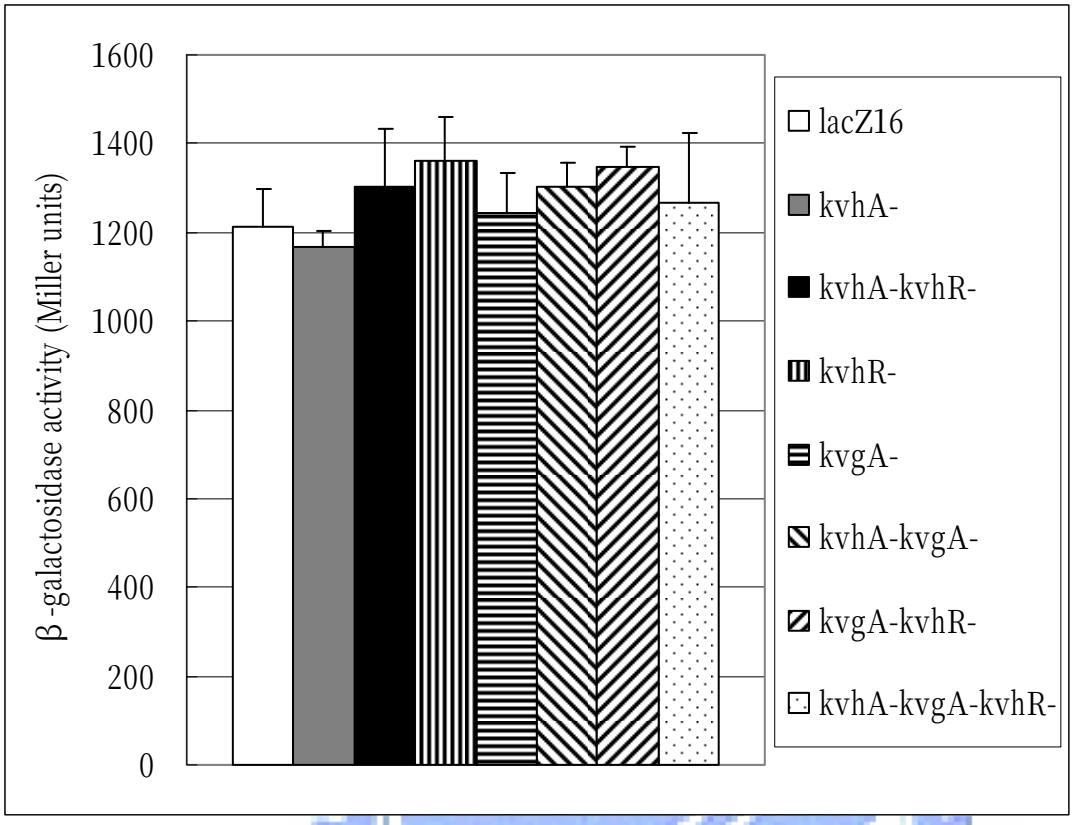
β -galactosidase activity (Miller units)
1600
1400
1200
1000
800
600
400
200
0
lacZ16
kvhA-
kvhA-kvhR-
kvhR-
kvgA-
kvhA-kvgA-
kvgA-kvhR-
kvhA-kvgA-kvhR-

(D)

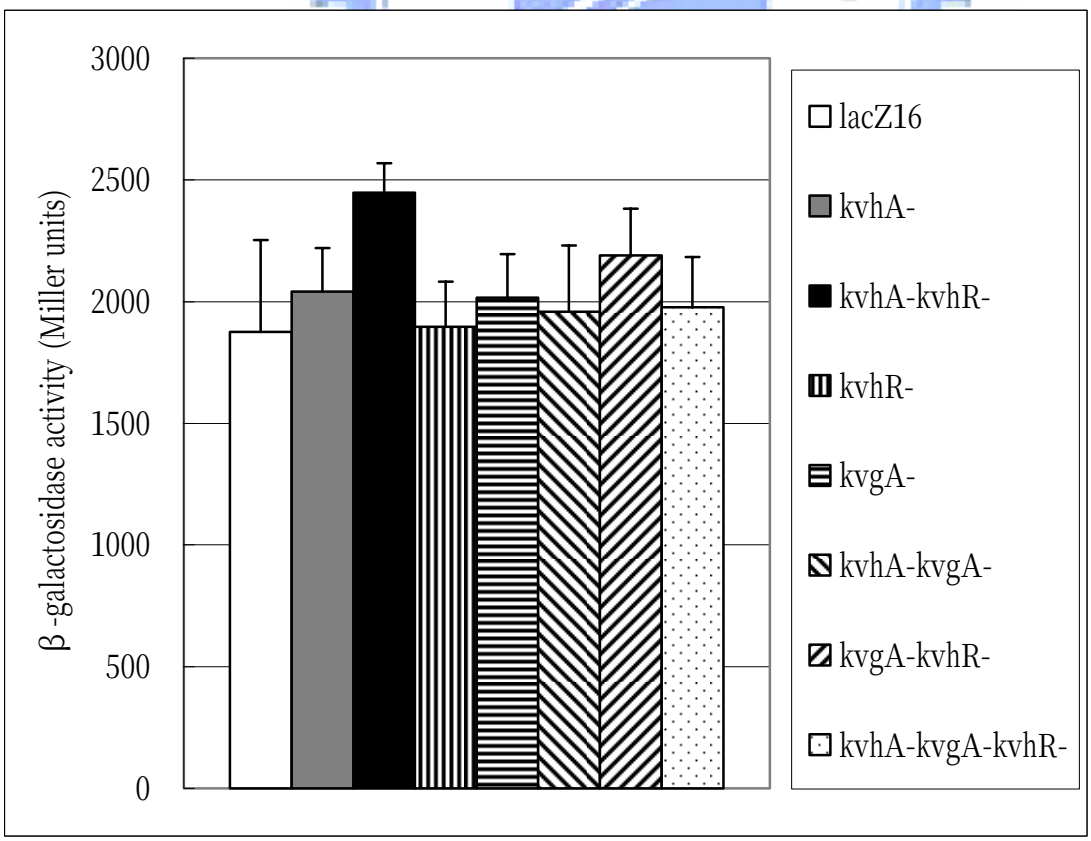
β -galactosidase activity (Miller units)
3000
2500
2000
1500
1000
500
0
lacZ16
kvhA-
kvhA-kvhR-
kvhR-
kvgA-
kvhA-kvgA-
kvgA-kvhR-
kvhA-kvgA-kvhR-

(E)

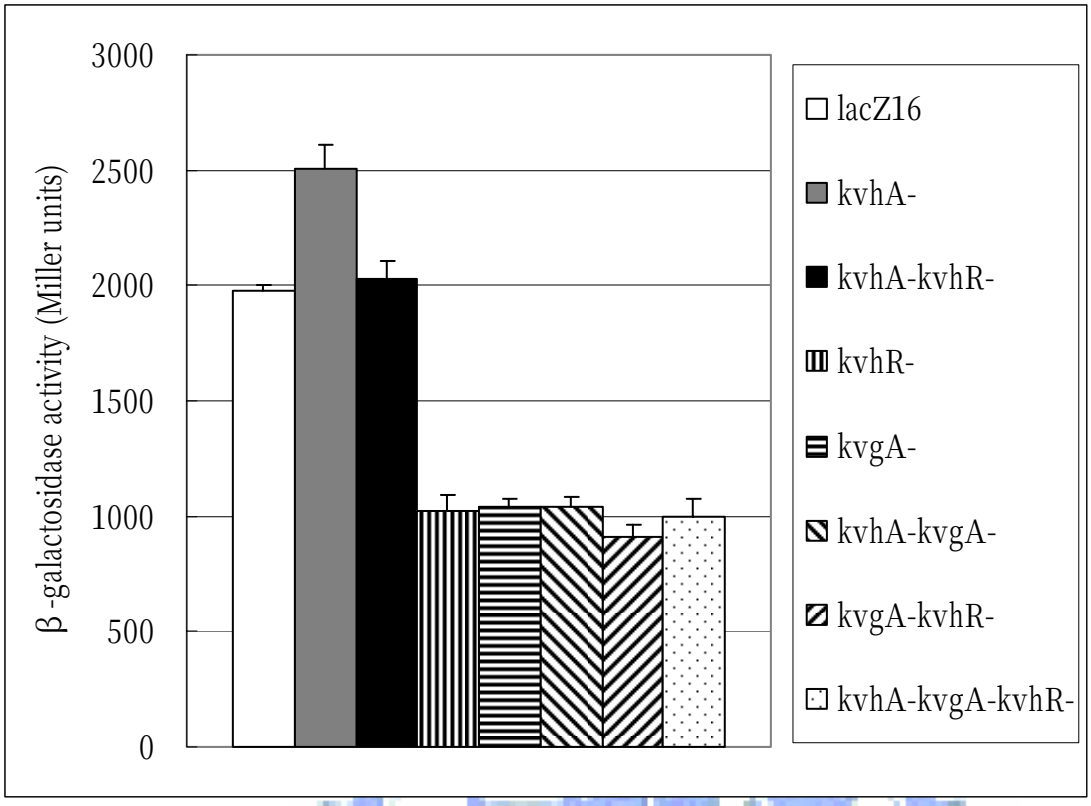

Fig. 10. The effects of *kvhA*, *kvgA* and *kvhR* mutations on the putative promoters of *K. pneumoniae* K2 *cps* genes. The β-galactosidase activities of porf1Z15 (A), porf2Z15 (B), porf3Z15 (C), porf4Z15 (D), and porf162Z15 (E) were measured at late log phase. The mean and standard deviation were calculated from three independent experiments.

(A)

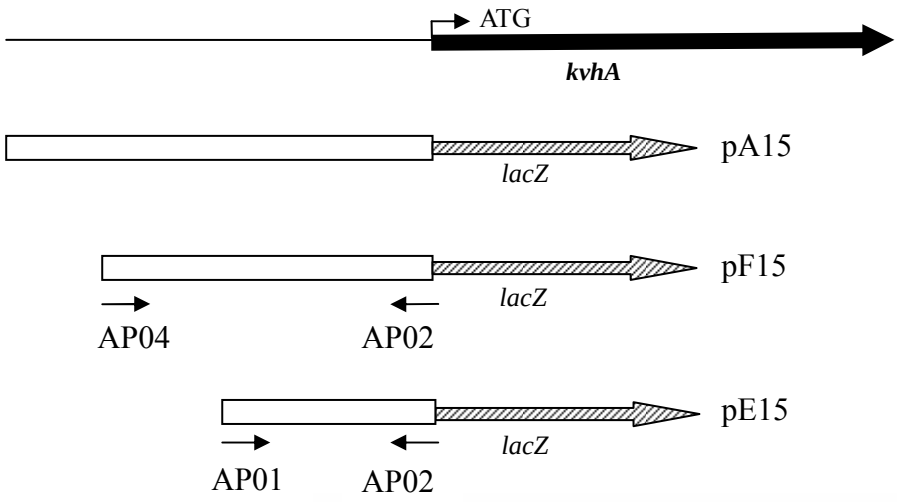

(B)

pA15

-476 AGGCGCGCGGATCCAGTTGCAGATAATCCTGACAGCGCATCA

-434 TATCTCGGGTCCGCGCCTCATCGGGGACGACATCCTTTCCCA

-392 CCGCGGCGCAACTCATTGCCAGTACTGTTATTCCTGCCATCA

pF15

-350 GATGTTTCCAAACCCATTTTCGCCAGAAGGCGCGTTTTTCTT

-308 TCGCCATTGTTATTATTTTACCTGCCAGTTGTCGCCGGACGA

-10

-266 TATTCCCGAGAGCTCACCTTAATAAGAGCAGATTAATCGTTT

-224 GCATTTTTTTTAACAGCAGACCGCGCTGAAGCAAGTGAACGC

pE15

-182 CCGTTCCTACAGCTGTCATCCAGCTATGCAAATATATTCGTC

-140 TGGCTCAGCTCCACAATATTTCCCTGGCCCAAAACGATTTGT

-98 GTTACAATTACGCCTTATAACGGCATCGATAAAAATAACCCC

-56 CGCCGCACCTGCACCAGGCATCGCCCTTCTTTTTTCATATCA

-14 GGATTTACGCCCCC**ATG**

Fig. 11. Mapping of the putative promoter regions of *kvhAS*. (A) Three *lacZ* transcriptional fusion clones, pA15, pE15 and pF15, were mad by cloning of different length of the upstream non-translated region of *kvhAS* into placZ15 and the primers used for PCR amplification used in this study are also indicated. (B) Nucleotide sequence of *kvhAS* upstream non-translated region. The arrows indicate the start sites of putative promoters and the predicted RpoS binding site is underlined.

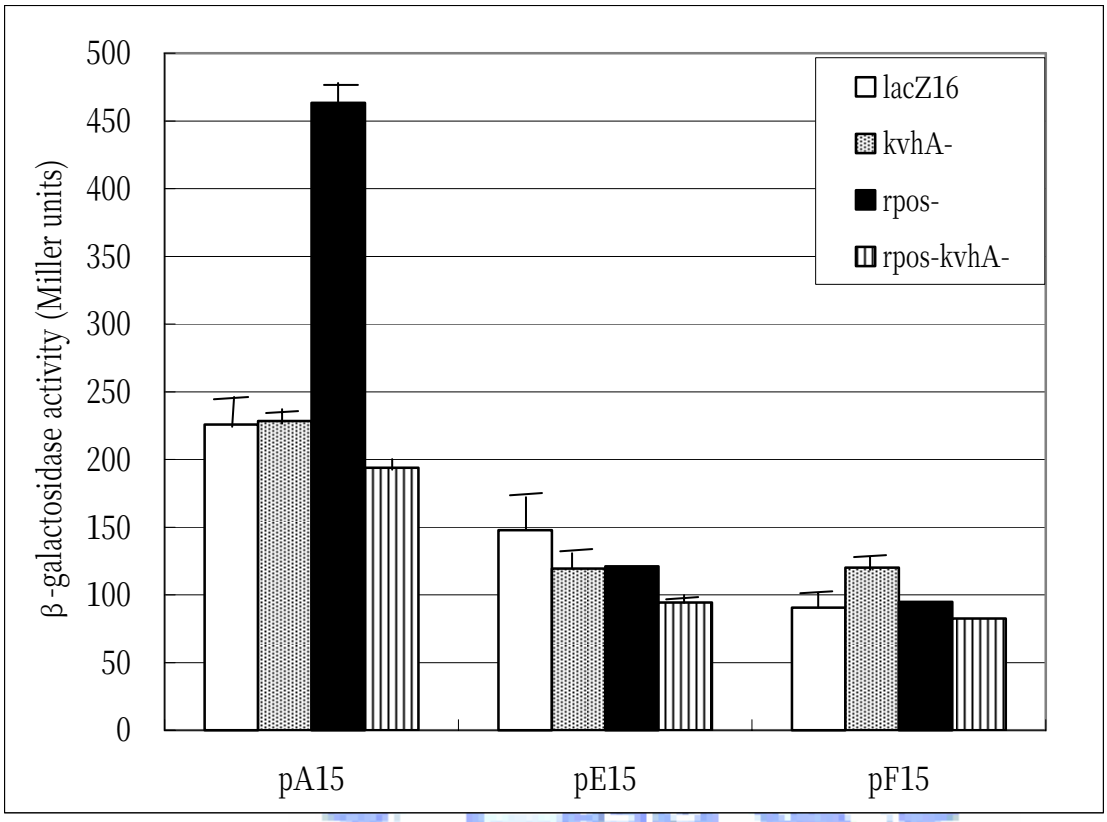

Fig. 12. Effects of the *rpoS* and *kvhA* mutations on the transcriptional activity of the putative promoter regions of *kvhAS*. The β-galactosidase activities were measured in the bacteria at late log phase. The mean and standard deviation were calculated from three independent experiments.

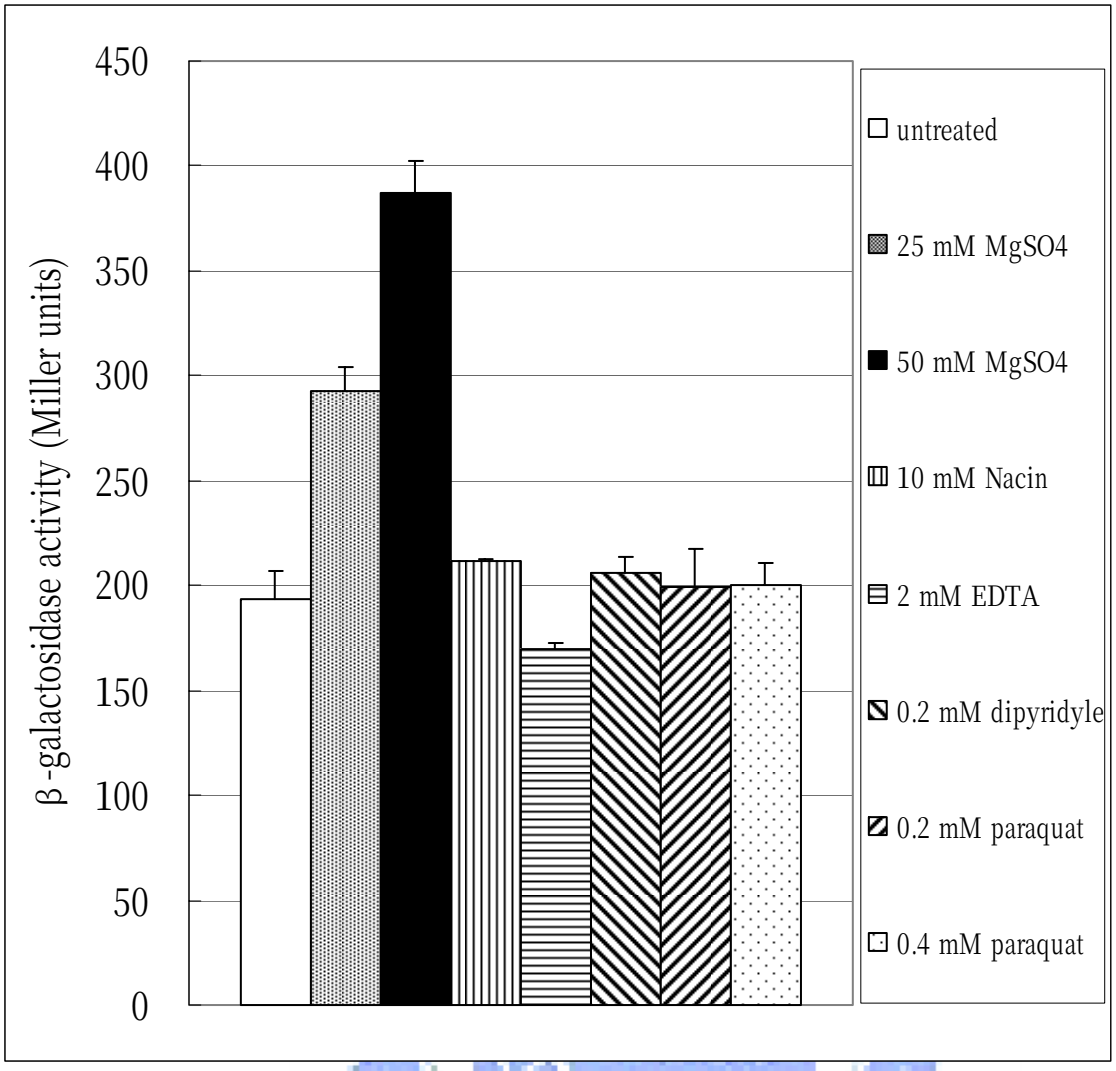

Fig. 13. The transcriptional activities of *kvhAS* promoter (pA15) were analyzed in wild-type LacZ16 under the treatment of several signal molecules. The bacteria were inoculated in M9 medium and cultured to early log phase (OD_{600}=0.4), then incubated with different reagents at 37℃ for 1 h prior to the test.

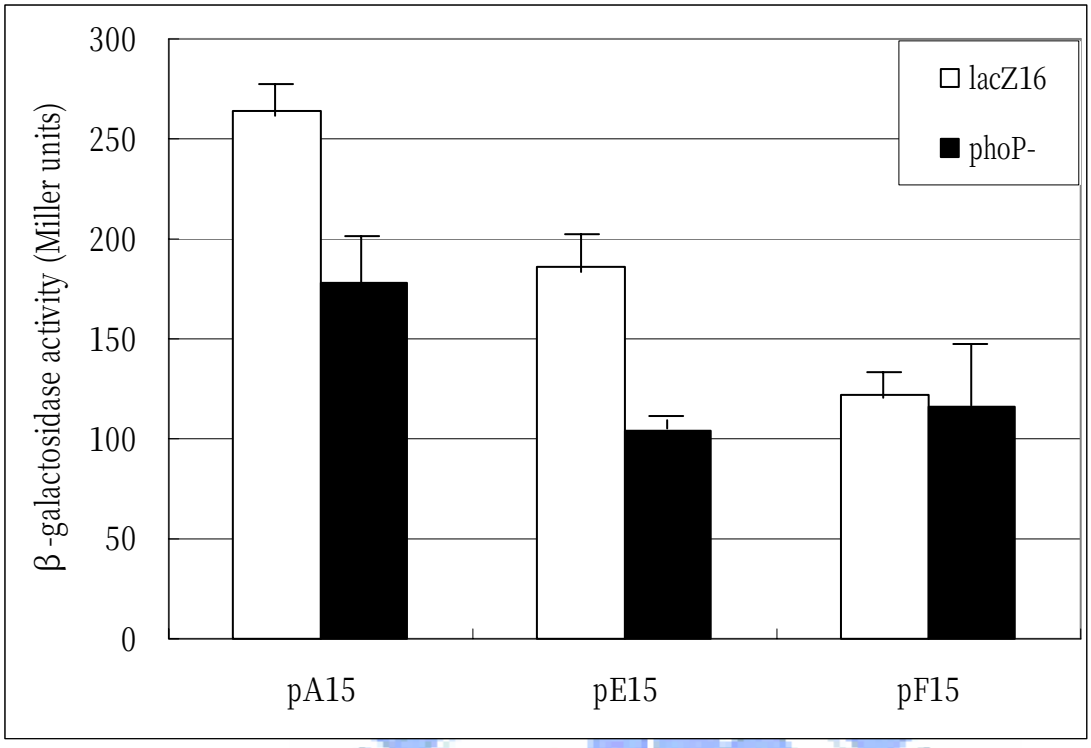

Fig. 14. Effect of the *phoP* mutation on the transcriptional activity of the putative promoter regions of *kvhAS*. The β-galactosidase activities were measured in the bacteria at late log phase. The mean and standard deviation were calculated from three independent experiments.

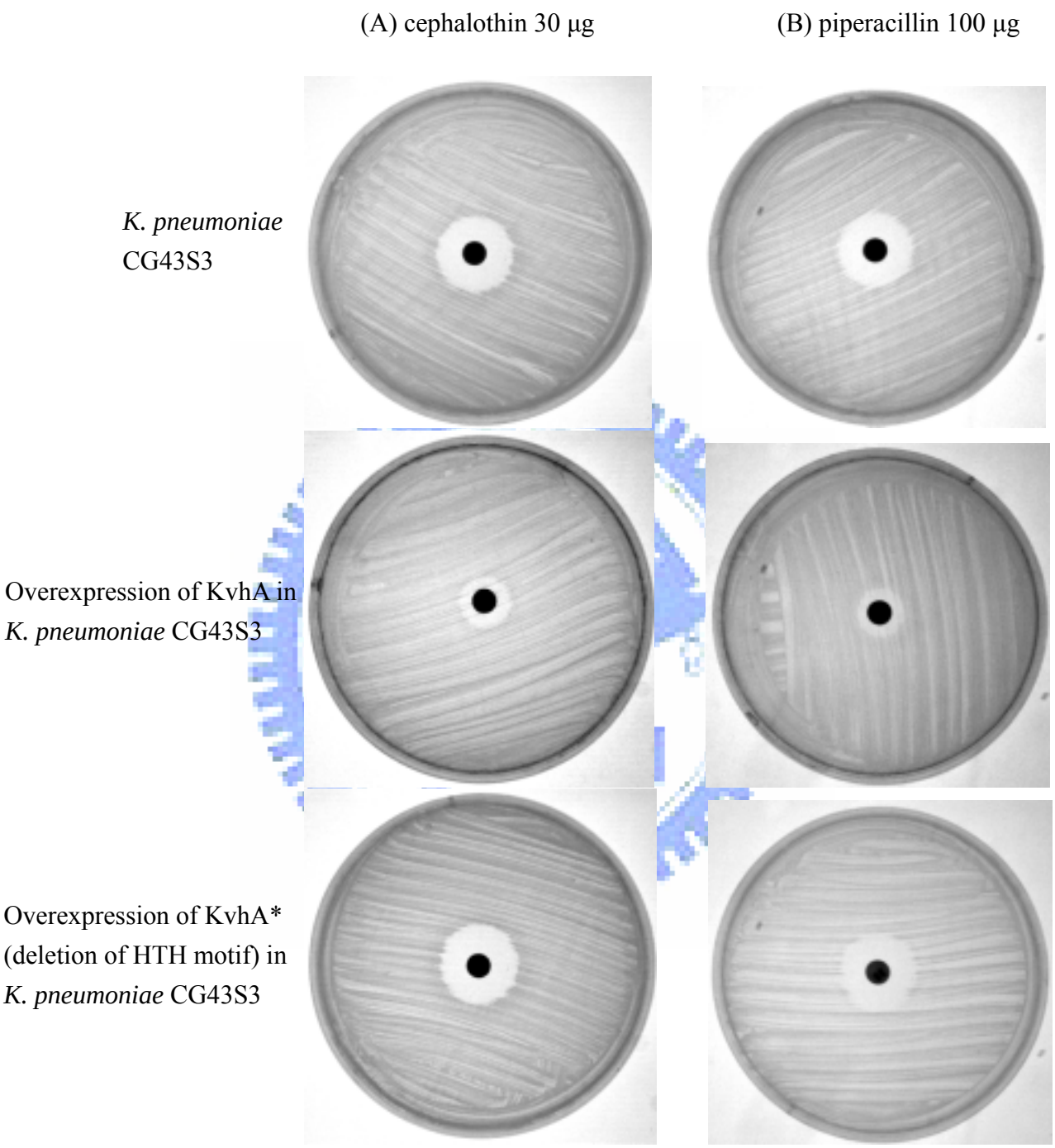
(A) cephalothin 30 μg
(B) piperacillin 100 μg
K. pneumoniae CG43S3
Overexpression of KvhA in K. pneumoniae CG43S3
Overexpression of KvhA* (deletion of HTH motif) in K. pneumoniae CG43S3

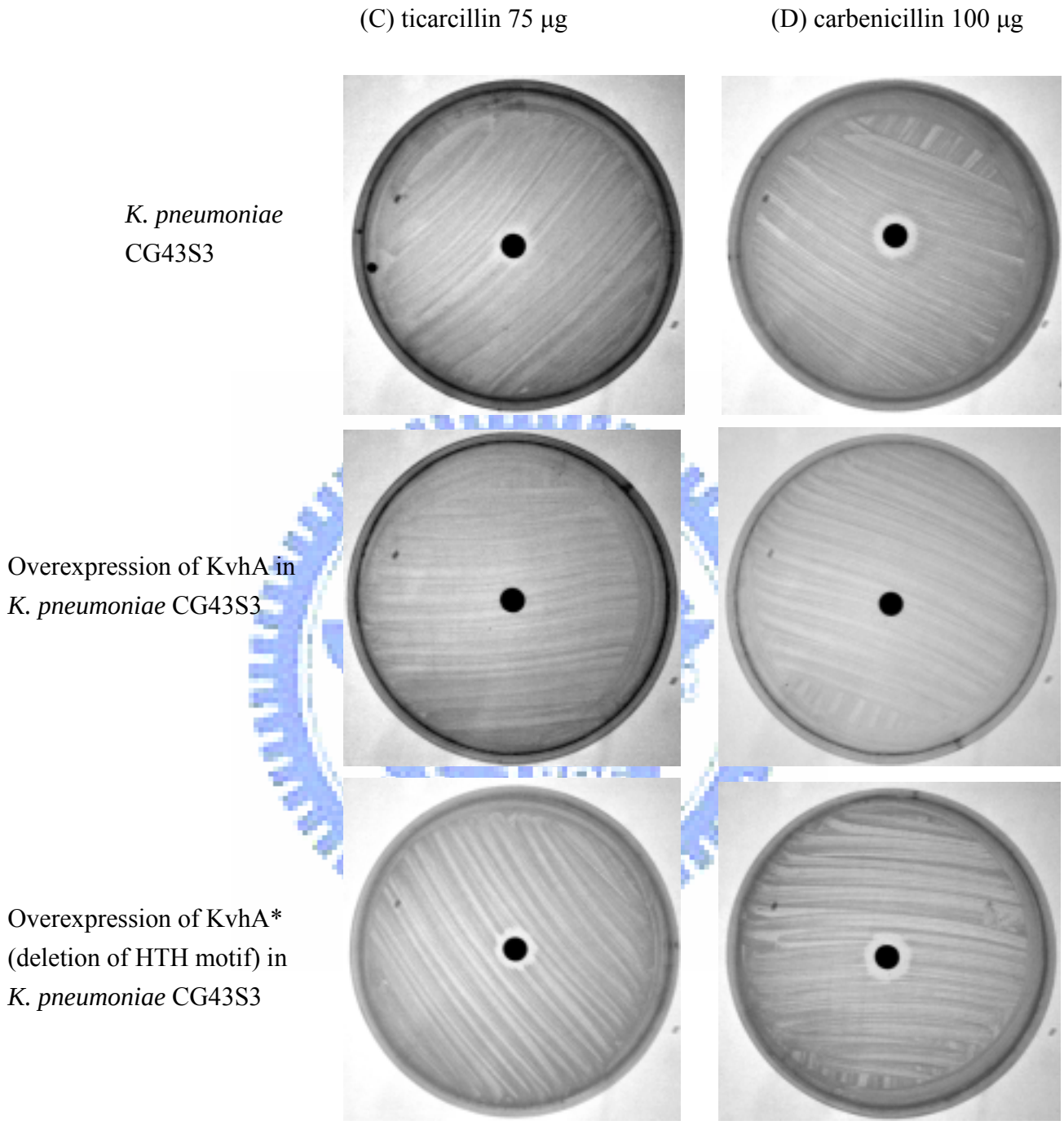
(C) ticarcillin 75 μg
(D) carbenicillin 100 μg
K. pneumoniae CG43S3
Overexpression of KvhA in K. pneumoniae CG43S3
Overexpression of KvhA* (deletion of HTH motif) in K. pneumoniae CG43S3

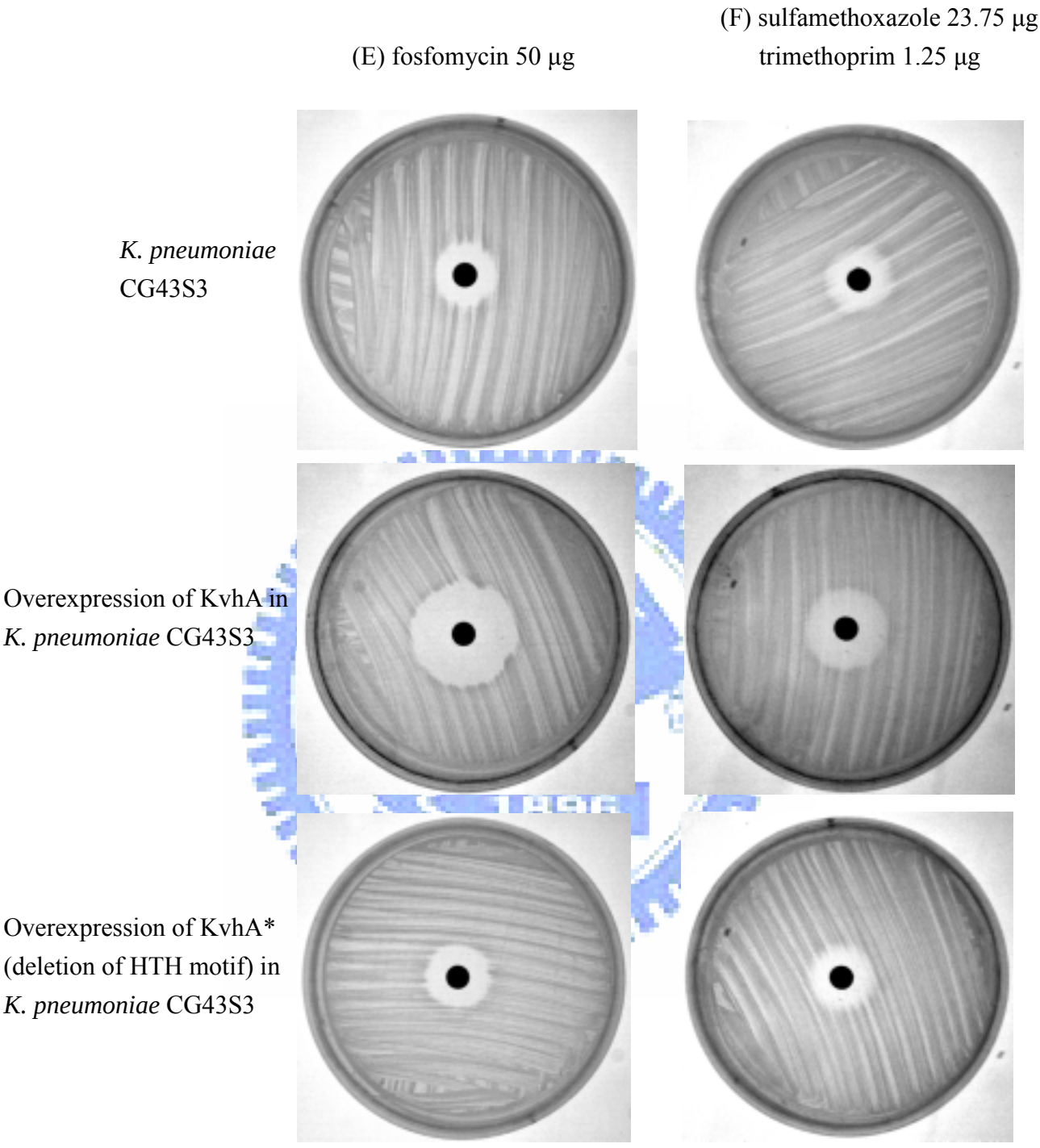

Fig. 15. Effect of KvhA overexpression on bacterial resistance activity to antibiotics. An overnight culture of bacteria was spread onto LB agar, then disks were placed onto the plates and zones of inhibition were measured after 16 h of incubation at 37°C. The following disc concentrations were used: (A) cephalothin 30 μg; (B) piperacillin 100 μg; (C) ticarcillin 75 μg; (D) carbenicillin 100 μg; (E) fosfomycin 50 μg; (F) sulfamethoxazole 23.75 μg + trimethoprim 1.25 μg.

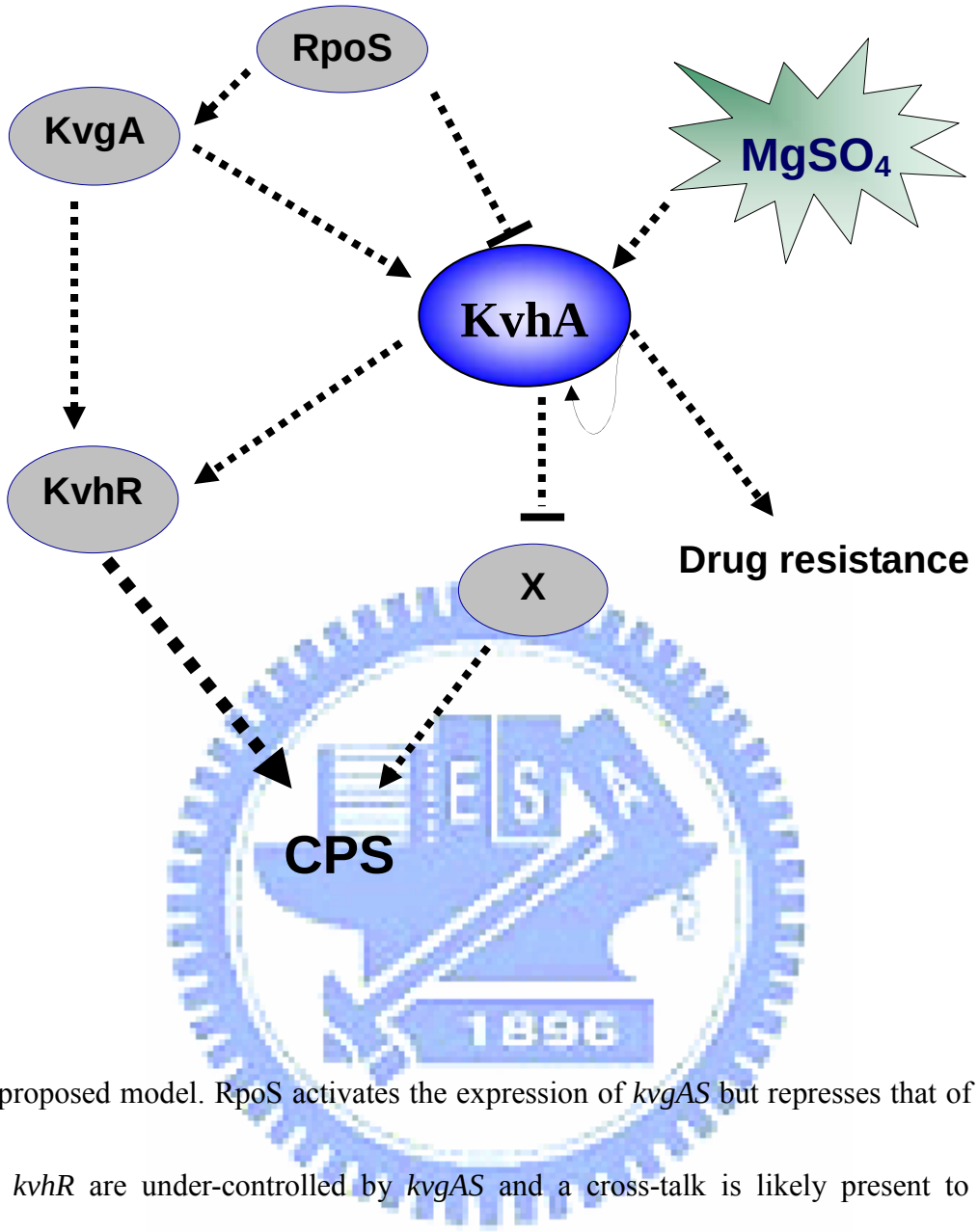

Fig. 16. A proposed model. RpoS activates the expression of *kvgAS* but represses that of *kvhAS*. Both *kvhAS* and *kvhR* are under-controlled by *kvgAS* and a cross-talk is likely present to regulate the bacterial CPS synthesis and LPS modification. A high-level concentration of Mg^{2+} is the signaling molecule for KvhAS expression and the expression of KvhAS affects the drug susceptibility.